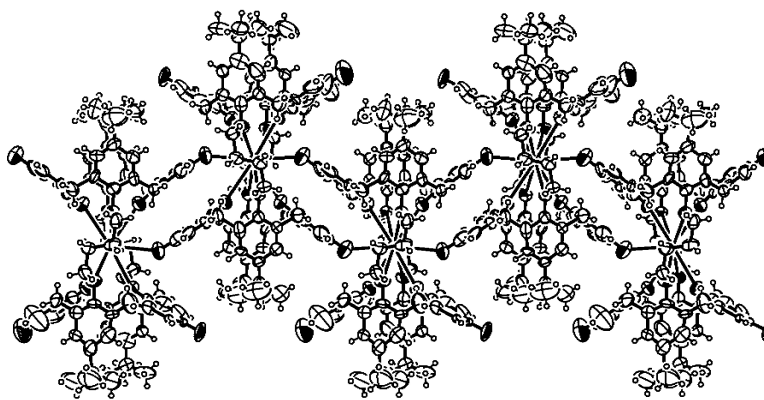


Bis(calix[4]diquinone) Receptors: Cesium- and Rubidium-Selective Redox-Active Ionophores

Philip R. A. Webber, Paul D. Beer, George Z. Chen, Vitor Felix, and Michael G. B. Drew

J. Am. Chem. Soc., **2003**, 125 (19), 5774-5785 • DOI: 10.1021/ja029740t • Publication Date (Web): 19 April 2003

Downloaded from <http://pubs.acs.org> on March 26, 2009



More About This Article

Additional resources and features associated with this article are available within the HTML version:

- Supporting Information
- Links to the 5 articles that cite this article, as of the time of this article download
- Access to high resolution figures
- Links to articles and content related to this article
- Copyright permission to reproduce figures and/or text from this article

[View the Full Text HTML](#)

Bis(calix[4]diquinone) Receptors: Cesium- and Rubidium-Selective Redox-Active Ionophores

Philip R. A. Webber,[†] Paul D. Beer,^{*,†} George Z. Chen,[§] Vitor Felix,^{‡,||} and Michael G. B. Drew[‡]

Contribution from the Department of Chemistry, Inorganic Chemistry Laboratory, University of Oxford, South Parks Road, Oxford OX1 3QR, United Kingdom, Department of Chemistry, University of Reading, Whiteknights, Reading, Berks, RG6 6AD, United Kingdom, and Department of Materials Science and Metallurgy, University of Cambridge, Pembroke Street, Cambridge, CB2 3QZ, United Kingdom

Received December 13, 2002; E-mail: paul.beer@chem.ox.ac.uk

Abstract: A new class of redox-active ionophore comprised of two calix[4]diquinone moieties connected through either alkylene or pyridylene linkages has been developed. Spectroscopic and electrochemical investigations, X-ray crystal structure analyses, and molecular modeling studies show butylene- and propylene-linked members of this family of redox-active receptors exhibit remarkable selectivity preferences and substantial electrochemical recognition effects toward cesium and rubidium cations.

Introduction

The development of molecular receptors designed to selectively recognize and sense charged or neutral guest species of biological and environmental importance is a highly topical research field.¹ A number of research groups have incorporated redox-active transition metal and organic centers into a variety of frameworks based on crown ethers, cryptands, and calixarenes and have shown some of these systems to be selective and electrochemically responsive to the binding of metal cations, particularly lithium,² sodium,³ and potassium.⁴ However, the construction of redox-active ionophores for the selective recognition of the larger rubidium and cesium metal cations has not, to our knowledge, been reported, a fact which is surprising in view of the environmental concern for monitoring radioactive cesium in nuclear waste solutions⁵ and the potential use of rubidium isotopes in radiopharmaceutical reagents.⁶

Significant research into the targeted binding of these larger group 1 cations has focused on the development of isoguanosine

aggregates⁷ and functionalized calix[4]arenes. Of the latter, highly stable complexes are formed between the rubidium cation and calixspherand hosts,⁸ while the 1,3-alternate calix[4]crown series of ligands bearing either one or two crown-6 units display exceptionally high Cs⁺/Na⁺ selectivities.⁹ Recent studies have described the application of modified calix[4]crown-6 hosts in cesium ion selective optical¹⁰ and microcantilever-based sensors.¹¹

In this paper, we report a new class of ionophore, the bis-(calix[4]diquinone), a series of redox-active receptors consisting of two calix[4]diquinone moieties connected by either alkylene or pyridylene spacer units. The combination of spectroscopic and electrochemical investigations, X-ray crystal structure analyses, and molecular modeling studies reveals certain members of this family of redox-active receptors exhibit remarkable selectivity preferences and substantial electrochemical recognition effects toward cesium and rubidium cations. The length and nature of the bridging spacer units between the two calix[4]diquinone moieties critically dictate the selectivity and strength of binding for group 1 metal cations.¹²

[†] University of Oxford.

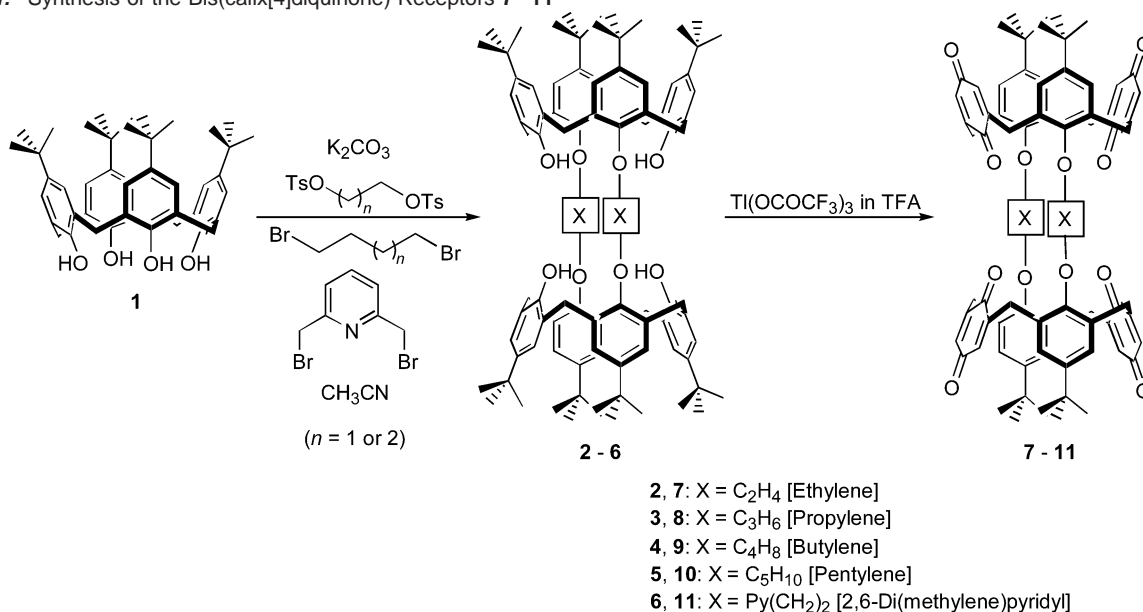
[‡] University of Reading.

[§] University of Cambridge.

^{||} On sabbatical leave from the Departamento de Quimica, Universidade de Aveiro, P-3810-193 Aveiro, Portugal.

- (1) (a) Beer, P. D.; Gale, P. A.; Chen, G. Z. *Adv. Phys. Org. Chem.* **1998**, *31*, 1. (b) Beer, P. D.; Gale, P. A.; Chen, G. Z. *J. Chem. Soc., Dalton Trans.* **1999**, 1897. (c) For a recent general review of luminescent sensors, see: Fabbrizzi, L., Ed. *Coord. Chem. Rev.* **2000**, *205*, 1.
- (2) (a) Plenio, H.; Diodone, R. *Inorg. Chem.* **1995**, *34*, 3964. (b) Plenio, H.; Aberle, C. *Organometallics* **1997**, *16*, 590.
- (3) (a) Shephard, D. S.; Johnson, B. F. G.; Matters, J.; Parsons, S. *J. Chem. Soc., Dalton Trans.* **1998**, 2289. (b) Medina, J. C.; Goodnow, T. T.; Rojas, M. T.; Atwood, J. L.; Lynn, B. C.; Kaifer, A. E.; Gokel, G. W. *J. Am. Chem. Soc.* **1992**, *114*, 10583.
- (4) (a) Beer, P. D.; Gale, P. A.; Chen, Z.; Drew, M. G. B.; Heath, J. A.; Ogden, M. I.; Powell, H. R. *Inorg. Chem.* **1997**, *36*, 5880. (b) Bourgeois, J.-P.; Echegoyen, L.; Fibboli, M.; Pretsch, E.; Diederich, F. *Angew. Chem., Int. Ed.* **1998**, *37*, 2118.
- (5) *Radioactive Waste Management and Disposal*; Cecille, L., Ed.; Elsevier: New York, 1991.
- (6) Anderson, C. J.; Welch, M. J. *Chem. Rev.* **1999**, *99*, 2219.

- (7) (a) Davis, J. T.; Tirumala, S. K.; Marlow, A. L. *J. Am. Chem. Soc.* **1997**, *119*, 5271. (b) Cai, M.; Marlow, A. L.; Fettinger, J. C.; Fabris, D.; Haverlock, T. J.; Moyer, B. A.; Davis, J. T. *Angew. Chem., Int. Ed.* **2000**, *39*, 1283.
- (8) Dijkstra, P. J.; Bruinink, J. A. J.; Bugge, K.-E.; Reinhoudt, D. N.; Harkema, S.; Ungaro, R.; Ugozzoli, F.; Ghidini, E. *J. Am. Chem. Soc.* **1989**, *111*, 7567.
- (9) (a) Ungaro, R.; Casnati, A.; Ugozzoli, F.; Pochini, A.; Dozol, J.-F.; Hill, C.; Rouquette, H. *Angew. Chem., Int. Ed. Engl.* **1994**, *33*, 1506. (b) Casnati, A.; Pochini, A.; Ungaro, R.; Ugozzoli, F.; Arnaud, F.; Fanni, S.; Schwing, M.-J.; Egberink, R. J. M.; de Jong, F.; Reinhoudt, D. N. *J. Am. Chem. Soc.* **1995**, *117*, 2767. (c) Thuéry, P.; Nierlich, M.; Lamare, V.; Dozol, J.-F.; Asfari, Z.; Vicens, J. *J. Inclusion Phenom. Macrocyclus Chem.* **2000**, *36*, 375.
- (10) Ji, H.-F.; Brown, G. M.; Dabestani, R. *Chem. Commun.* **1999**, 609.
- (11) Ji, H.-F.; Finot, E.; Dabestani, R.; Thundat, T.; Brown, G. M.; Britt, P. F. *Chem. Commun.* **2000**, 457.
- (12) Part of this work has been published as a preliminary communication: Webber, P. R. A.; Chen, G. Z.; Drew, M. G. B.; Beer, P. D. *Angew. Chem., Int. Ed.* **2001**, *40*, 2265.

Scheme 1. Synthesis of the Bis(calix[4]diquinone) Receptors 7–11

Synthesis

The novel bis(calix[4]diquinone) receptors were prepared via the initial syntheses of various bis(calix[4]arene) derivatives¹³ connected by alkylene chain and pyridylene spacer units, and subsequent oxidation of the remaining phenolic groups to quinone moieties. The resulting redox-active ionophores contain a three-dimensional array of eight oxygen donor atoms. By varying the length and nature of the connecting spacer units, we achieved the selective recognition and electrochemical sensing of cesium and rubidium group 1 metal cations.

Reaction of a suspension of *p*-*tert*-butylcalix[4]arene **1** and potassium carbonate in acetonitrile with ethane-1,2-ditosylate, propane-1,3-ditosylate, 1,4-dibromobutane, 1,5-dibromopentane, or 2,6-bis(bromomethyl)pyridine gave the bis(calix[4]arene) derivatives **2–6** in yields ranging from 23% to 53% (Scheme 1). Oxidation of these compounds with thallium tris(trifluoroacetate), Tl(OCOCF₃)₃, in trifluoroacetic acid^{4a,14} gave the new bis(calix[4]diquinone) ionophores **7–11** in yields of 8%, 28%, 10%, 9%, and 18%, respectively, after column chromatography and recrystallization. All of the intermediates and bis(calix[4]diquinone) receptors discussed have been characterized using ¹H and ¹³C NMR, electrospray or FAB mass spectrometry, and microanalysis.

Solid State Structures of 3 and Bis(calix[4]diquinone) 10

Crystals of **3** suitable for X-ray diffraction were grown by layering a chloroform solution of the ligand with methanol, and its structure is shown in Figure 1. The two calix[4]arene moieties within the molecule adopt regular cone conformations, a consequence of hydrogen bond formation between proximal –OH and –OR groups. The precise conformation of each calix-

[4]arene can be accurately described by the angles made by the four phenyl rings with the plane of the four methylene groups, and these values are 58.6°, 60.5°, 61.9°, 61.2° and 59.6°, 62.9°, 59.9°, 63.2°, respectively. Overall, the two calix[4]arene units are off-parallel, with there being an angle of 14.9° between the planes created by their respective methylene bridges. The propylene linkages each show four *trans* torsion angles; thus, the central angles in the C(26)–O(250)–C(251)–C(252)–C(253)–O(650)–C(66) linkage are –170.4°, 179.3°, –175.6°, and 170.7°, and in the C(46)–O(450)–C(451)–C(452)–C(453)–O(850)–C(86) linkage they are 167.0°, –174.8°, –179.4°, and –179.3°, respectively.

Crystals of bis(calix[4]diquinone) **10** were grown by slow evaporation from a solution of the ligand in dichloromethane/DMSO. The structure of **10** contains a crystallographic center of symmetry and is shown in Figure 2. Each calix[4]diquinone adopts the 1,3-alternate conformation with the *tert*-butyl groups directed outward from the center of the dimer. The planes created by opposite diquinone units intersect each other at 40.8°, and those of the two phenyl rings intersect at 59.6°; thus, all rings are within 30° of the central axis. Torsion angles for atoms C(26)–O(250)–C(251)–C(252)–C(253)–C(254)–C(255)–O(450)–C(46) in the pentane link are –73.2°, –171.0°, –173.5°, –172.4°, 57.3°, and 162.2°, respectively, thus demonstrating a –gttgt conformation (g = gauche, t = trans) around the six central bonds. As is apparent from the figure, the central cavity is too small to contain a metal ion in this conformation. The bis(calix[4]diquinone) contains two dimethylsulfoxide molecules. These are positioned within the cavity of each calix[4]diquinone with the methyl groups directed toward the center of the macrocycle. There are close contacts between the hydrogen atoms of the solvent methyl groups and the quinone oxygen atoms (2.87, 2.89, 3.24 Å) and also toward the phenyl rings of the macrocycle (3.11, 3.23 Å).

Variable-Temperature ¹H NMR Studies

The room-temperature ¹H NMR spectra of **7–10** in CDCl₃ exhibit AB splitting patterns of the ArCH₂Qu protons consistent with cone conformations for the calixarenes. However, for the

- (13) For a review of bis- and multiple calixarenes, see: Saadioui, M.; Böhmer, V. In *Calixarenes 2001*; Asfari, Z., Böhmer, V., Harrowfield, J., Vicens, J., Eds.; Kluwer Academic: Dordrecht, The Netherlands, 2001; Chapter 7, p 130.
- (14) (a) McKillop, A.; Swann, B. P.; Taylor, C. C. *Tetrahedron* **1970**, *26*, 4031. (b) Reddy, P. A.; Kashyap, R. P.; Watson, W. H.; Gutsche, C. D. *Isr. J. Chem.* **1992**, *32*, 89. (c) Reddy, P. A.; Gutsche, C. D. *J. Org. Chem.* **1993**, *58*, 3245.

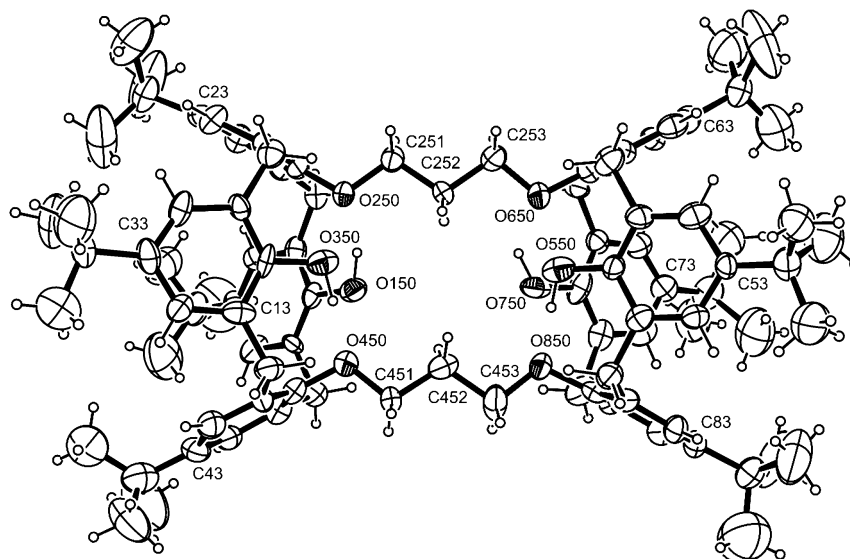


Figure 1. Crystal structure of bis(calix[4]arene) **3** in $3 \cdot 3\text{CHCl}_3 \cdot 1.5\text{H}_2\text{O}$ with ellipsoids at 30% probability. The chloroform and water molecules are not shown.

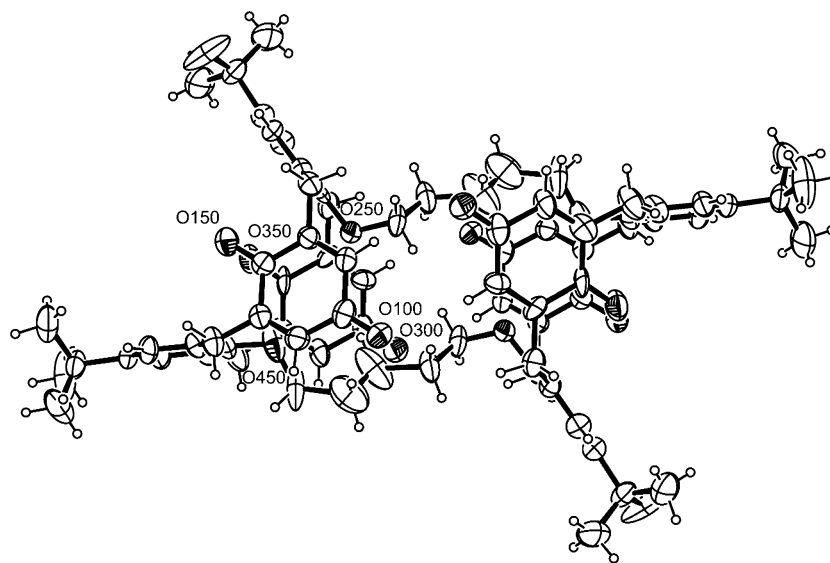


Figure 2. Plot of the crystal structure of bis(calix[4]diquinone) **10** in $10 \cdot 4\text{DMSO}$ with ellipsoids at 30% probability. The DMSO solvent molecules have been omitted.

pyridylene-bridged host **11**, a 1,3-alternate conformation is adopted in CDCl_3 solution. Low-temperature ^1H NMR studies of the propylene-linked species **8** in CD_2Cl_2 solution revealed that, on cooling, all resonances broaden, and the *tert*-butyl resonance splits into several peaks. This suggests either that the two calix[4]diquinones within the molecule adopt different or nonequivalent conformations or that there are two or more different overall conformations in solution. Unfortunately, the precise conformation of **8** is unclear due to the broadness of the spectrum even at 193 K. Similar dynamic processes have been observed with alkyl and ester lower rim substituted calix[4]diquinones.^{4a,15}

Stability Constant Determinations by UV/Vis Titration Experiments

UV/Vis titration experiments were undertaken on the bis-(calix[4]diquinone) receptors by monitoring the perturbation of the $n \rightarrow \pi^*$ electronic transition of the quinone moiety on addition of alkali metal cation guest. With **8** and **9**, titrations

were undertaken in a highly competitive solvent mixture of 99:1 DMSO:water. Weaker group 1 metal binding was observed with **10** and **11**, and, as a consequence, relatively less competitive solvent media were used for the titration experiments with these receptors. The stability constants for 1:1 complexes were then calculated using the Specfit program.¹⁶ The data obtained (Table 1) reveal that **8** forms a strong selective complex with rubidium cations and exhibits the selectivity trend $\text{Rb}^+ > \text{Cs}^+ > \text{K}^+ \gg \text{Na}^+$. In contrast, **9** containing butylene spacers exhibits a remarkably high selectivity for cesium ions; in fact, in this competitive aqueous DMSO solvent mixture, **9** does not form complexes with either sodium or potassium cations.¹⁷ This very high Cs^+/Na^+ selectivity preference is of real significance for

(15) Casnati, A.; Comelli, E.; Fabbi, M.; Bocchi, V.; Mori, G.; Ugozzoli, F.; Lanfredi, A. M. M.; Pochini, A.; Ungaro, R. *Recl. Trav. Chim. Pays-Bas* **1993**, *112*, 384.

(16) Binstead, R. A.; Zuberbühler, A. D. Specfit Global Analysis, Version 2.90X.

(17) UV/Vis experiments of **9** in 1:1 dichloromethane:DMSO revealed that the receptor selectively responded to cesium cation in the presence of a 75-fold excess of sodium cations.

Table 1. Stability Constant Data^a for the Alkali Metal Complexes of **8–11**

| | KM^{-1} | | | |
|-----------------|-------------------|-------------------|-------------------|-------------------|
| | 8 ^b | 9 ^b | 10 ^c | 11 ^d |
| Na ⁺ | <i>e</i> | <i>e</i> | 3.2×10^4 | <i>e</i> |
| K ⁺ | 7.9×10^3 | <i>e</i> | 6.3×10^4 | 2.0×10^3 |
| Rb ⁺ | 6.3×10^4 | 40 | 2.5×10^4 | 5.0×10^3 |
| Cs ⁺ | 1.3×10^4 | 1.6×10^3 | 2.0×10^4 | 1.3×10^4 |

^a At 298 K. Maximum error estimated to be $\pm 10\%$. ^b Conducted in 99:1 DMSO:H₂O. ^c Conducted in 7:3 CHCl₃:CH₃OH. ^d Conducted in 1:1 CH₂Cl₂:DMSO. ^e No evidence of complexation was observed.

the separation of radioactive cesium from nuclear waste as such solutions typically contain sodium ions at high concentrations. It is noteworthy that by including one more carbon atom into the alkyl bridges, as in receptor **10**, the strength of cation complexation is greatly reduced and binding becomes nonselective. The introduction of pyridylene spacers, giving macrocycle **11**, allows for relatively strong ion complexation, a consequence of the enhanced rigidity of the linkages and the presence of two extra donor atoms. It shows a selectivity preference for the larger group 1 cations with the binding trend Cs⁺ > Rb⁺ > K⁺ >> Na⁺. However, its binding is weaker than that for either **8** or **9**, presumably due to the greater length of its bridging chains. Stability constant determinations were not conducted on **7** due to its poor solubility in all common solvents.

The data in Table 1 clearly show that the length of the spacer between the two calix[4]diquinone moieties crucially dictates the selectivity and strength of binding of alkali metal cations.¹⁸ Titration experiments were also conducted between receptor **8** and strontium and barium cations in 99:1 DMSO:water; however, for each group 2 metal, there was no evidence for complex formation.

Solid State Structure of 9·CsClO₄

The crystal structure of the cesium complex of **9** (Figure 3), reported previously,¹² has approximate two-fold symmetry. Both calix[4]diquinones have the well-known C₂ flattened-cone conformation with phenyl rings (1, 3, 5, and 7) almost perpendicular to the plane of the methylene rings, intersecting at angles of 87.5°, 86.5°, 89.1°, and 84.7°, respectively, while the four diquinone rings (2, 4, 6, and 8) intersect at angles of 35.0°, 35.0°, 29.8°, and 32.2°. The torsion angles for atoms Cn6–On50–Cn51–Cn52–Cn53–Cn54–On55–Cn56 in the butane links ($n = 1, 3$) between the two oxygen atoms of the calix[4]diquinones show angles of 171.0°, –65.7°, 176.9°, –72.3°, 172.2°, and 171.9°, –69.6°, 178.5°, –72.6°, 167.9°; thus, both display *t*–*gt*–*gt* conformations. The cesium atom is bonded to the eight oxygen atoms forming the central cavity with Cs–O distances of 3.224(8)–3.292(8) Å to the four diquinone oxygen atoms with longer distances to the four ether oxygen atoms (3.364(9)–3.530(10) Å). In addition, the cesium atom forms two strong bonds to adjacent oxygen atoms at the top rim of two neighboring molecules (O200, 3.226(8) Å (–*x*, –*y*, –*z*); and O400, 3.287(8) Å (–*x*, 1 – *y*, –*z*)), thus setting up a 1D polymeric chain parallel to the *y* axis. Furthermore, each quinone unit bearing a bonding *exo*-oxygen atom probably experiences a weak π – π stacking interaction with an analogous

quinone unit in a neighboring molecule. This is manifested in an average C···C bond distance of 3.66 Å and the two quinone moieties being slightly offset.

Molecular Mechanics Calculations of Macrocycle Hole Size

In an effort to explain the particular group 1 metal cation selectivities of the bis(calix[4]diquinone) receptors **8**, **9**, and **10**, molecular mechanics calculations were performed to determine macrocycle hole sizes.¹⁹ To calculate the hole size, the cone/cone (*c/c*) conformation for each receptor was used. The included metal cation was then constrained to be bonded to all eight oxygen atoms at a specific distance. As a result of the crystal structure of **9**·Cs⁺ showing metal to carbonyl oxygen bonds being shorter than those to ether oxygens, the latter bond distances were fixed at a length 0.2 Å greater. The eight M–O distances were then varied in 0.05 Å intervals between the limits of 2.45–3.85 Å. At each distance, the macrocycle energy is minimized via molecular mechanics, and the resulting energies, shown in Figure 4, therefore represent the steric strain in the macrocycle when complexing to a particular metal ion with a specific radius.

Receptor **9** carrying butylene chains displays a minimum steric energy at a M–O(carbonyl) distance of 3.12 Å, a value which, in part, explains the ligand's selectivity for cesium cation. Propylene-bridged host **8** shows a broad minimum at around 2.75–2.90 Å with two distinct conformations. This range of values is in accord with the experimentally observed rubidium ion selectivity. In contrast, receptor **10** shows a minimum at around 3.5 Å, a distance too great for effective alkali metal binding to occur. The discontinuities in this curve indicate variations in conformation. This calculation substantiates the finding that **10** only complexes group 1 cations weakly and with little selectivity. While molecular mechanics energies for different molecules cannot always be appropriately compared, it is probably significant that the energy of complexed **9** is less than that of either complexed **8** or **10**, indicating that this ligand is more suitable for metal cation binding, providing a cavity which is neither as small as **8** nor as large as **10**.

Molecular Dynamics Simulations on Macrocycles with Na⁺, K⁺, Rb⁺, and Cs⁺ Cations

Molecular dynamics simulations of macrocycles **8–10** with the four metal ions Na⁺, K⁺, Rb⁺, and Cs⁺ were carried out. For each system, the starting model was the lowest energy *c/c* conformation of the ML⁺ complex. The simulations were carried out at room temperature and continued for 500 ps. The resulting changes in conformation are described by the changes in the torsion angles in the alkylene links, illustrated for L·Rb⁺ in Figure 5, and the metal oxygen distances listed in Table 2.

There are significant conformational changes in **8** as shown in Figure 5a with torsion angles varying by up to 60°, although none change between *gauche* and *trans*. The overall conformation of the macrocycle remains *c/c*. For all four metals, there is a large difference between the M–O (carbonyl) and M–O (ether) distances, which is primarily a steric effect as the difference is larger for the smaller metals. The standard deviations for the bonds given in Table 2 give a clear indication

(18) Electrospray mass spectrometry competition experiments of **8–11** with group 1 metal iodides semiquantitatively reflected the results of the UV/vis titration experiments.

(19) Felix, V.; Costa, J.; Delgado, R.; Drew, M. G. B.; Duarte, M. T.; Resende, C. *J. Chem. Soc., Dalton Trans.* **2001**, 1462.

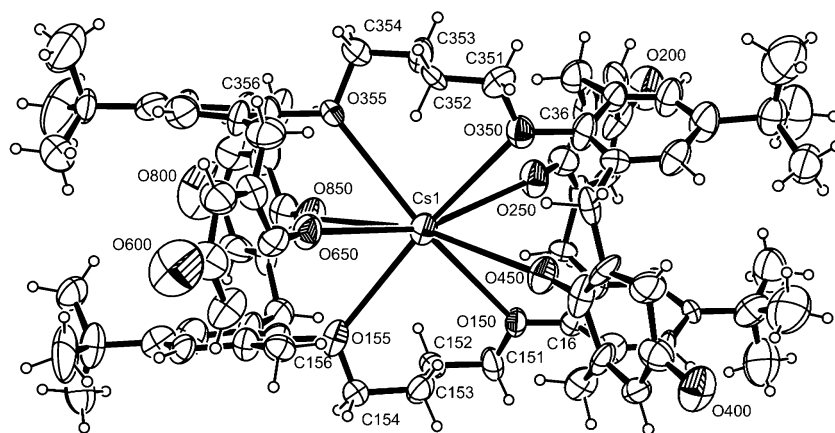


Figure 3. The structure of the cesium complex of bis(calix[4]diquinone) **9** in crystals of $9 \cdot 2\text{CH}_3\text{OH} \cdot 1.5\text{H}_2\text{O}$ with ellipsoids at 30% probability. The methanol and water solvent molecules are not shown.

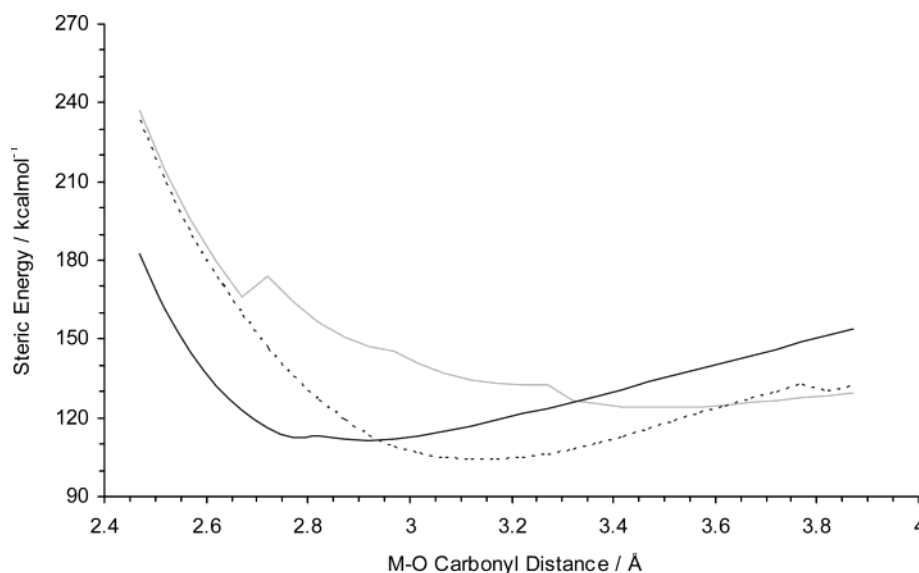


Figure 4. Plot of steric energy against M–O distance for macrocycles **8** (black continuous line), **9** (dotted line), and **10** (gray continuous line).

of whether all eight oxygen atoms are bonded to the metal. For example, the large standard deviations for Na^+ , particularly in **9** and **10**, show that the small metal ion can only bind to four or five oxygen atoms at any one time. With **8** and **9**, for K^+ , Rb^+ , and Cs^+ , the standard deviations for the bond lengths suggest that these metals can bind to the eight oxygen atoms within the macrocycles. However, with **10**, the standard deviations are very much larger, demonstrating that the macrocycle is not suited to encapsulate the metal ions with eight metal–oxygen bonds. For **9**, the plots of torsion angle against time show much less deviation than for **8**, or indeed **10**, confirming that this ligand is the best suited of the three to encapsulate a metal ion. As for **8**, while the mean M–O distances may be equivalent, their standard deviations are not, showing a much wider range for the smaller ions than for the cesium ion. The M–O distances in **9** are significantly larger than in **8**, a fact attributable to the more constricted nature of the smaller macrocycle.

There is more variation in the torsion angles of **10** than in **9**, showing that this ligand is more flexible and that the metal ion is less tightly bound. It is interesting that the mean M–O distances are comparable to those found in **9** and in some cases

smaller. There is a large difference between the average M–O (carbonyl) and M–O (ether) distances, which again is indicative of the asymmetric steric strain in the molecule.

Variable-Temperature ^1H NMR Studies of Cation Complexes

To account for the absence of binding by some of the bis(calix[4]diquinone) hosts with group 1 cations and also in an attempt to gain further solution evidence as to how different cations are bound in the cavity of the receptors, variable-temperature ^1H NMR experiments were undertaken. In theory, a metal cation could bind to all eight oxygen donor atoms simultaneously or be in a state of motion shuttling between the two calix[4]diquinone moieties within the molecule but only being coordinated to one calix[4]diquinone at any specific time, or be bound to both calix[4]quinones but not using all available oxygen donors.

The solvent choice for the VT experiments was limited as the solvent itself had to be weakly competitive to enable the sodium cation to be complexed, have a low freezing point, and be able to solubilize both the host, the guest, and the complex. Acetone- d_6 was found to satisfy all of these criteria.

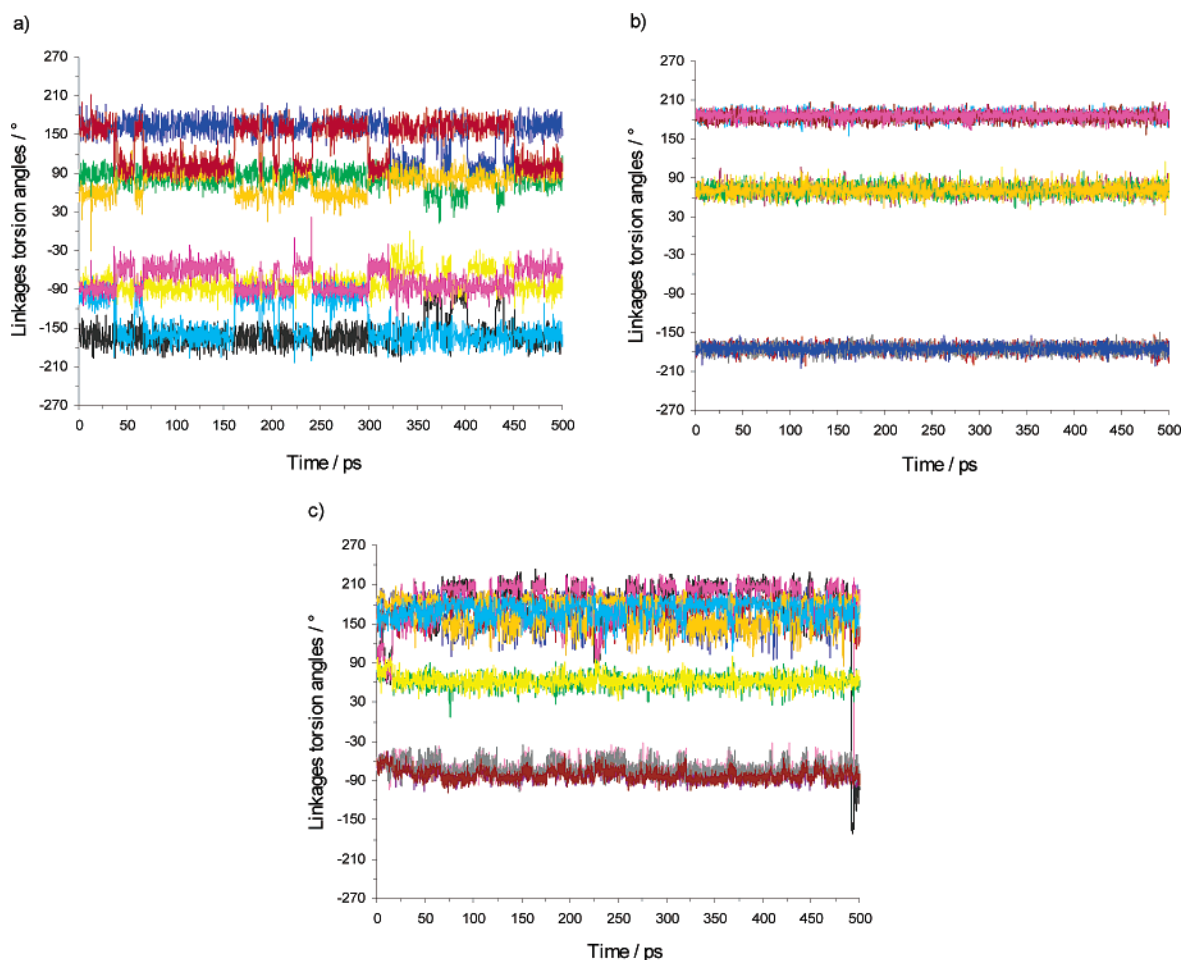


Figure 5. Variations in linkage torsion angles during the molecular dynamics simulations of (a) $8\cdot\text{Rb}^+$, (b) $9\cdot\text{Rb}^+$, and (c) $10\cdot\text{Rb}^+$. $\text{O}-\text{CH}_2-\text{CH}_2-\text{CH}_2$ and $\text{CH}_2-\text{CH}_2-\text{CH}_2-\text{CH}_2$ torsion angles are represented using the following color scheme: (a) black, yellow, green, blue from the first linkage and sky blue, pink, gold, red from the second linkage; (b) red, violet, gray, blue from the first linkage and sky blue, green, brown, gold, pink from the second linkage; (c) black, blue, rose, violet, green, red from the first linkage and pink, gold, gray, brown, yellow, sky blue from the second linkage. For the three macrocycles, the torsion angles (colors) of both linkages are listed sequentially and starting from the same calix[4]diquinone at the $\text{O}-\text{CH}_2-\text{CH}_2-\text{CH}_2$ torsion angle.

Table 2. Variations in M–O Distances during Molecular Dynamics Simulations of ML^+ at Room Temperature

| | mean M–O distance: carbonyl, ether/Å | | |
|---------------|--------------------------------------|--------------------|---------------------|
| | 8 | 9 | 10 |
| Na^+ | 2.63(32), 3.29(53) | 3.27(92), 3.61(81) | 3.00(63), 3.47(105) |
| K^+ | 2.73(15), 3.29(39) | 3.14(32), 3.54(36) | 3.06(61), 3.61(92) |
| Rb^+ | 2.79(14), 3.31(36) | 3.13(32), 3.53(36) | 3.16(40), 3.68(87) |
| Cs^+ | 2.88(12), 3.33(31) | 3.16(19), 3.54(27) | 3.34(49), 3.81(81) |

The first experiment compared the ^1H NMR spectra of $8\cdot\text{Na}^+$ with those of $8\cdot\text{Rb}^+$ in the temperature range from 318 to 193 K. Assuming that the cation is bound strongly to all donor sites and the complex is quite rigid, the proton spectrum of the complex would be expected to be invariant to temperature. This was indeed found to be the case for $8\cdot\text{Rb}^+$, the spectrum only slightly broadening as the temperature was lowered to 193 K. However, for $8\cdot\text{Na}^+$, the series of spectra at differing temperatures was very different (Figure 6).

Above approximately 273 K, the spectra are consistent with a time-averaged complex in which the sodium cation is mobile. As the temperature is lowered, new resonances begin to appear which sharpen significantly between 213 and 193 K, indicating the presence of an immobilized complex. The spectrum at 193 K is consistent with that of a symmetric molecule in which the

two calix[4]diquinones adopt partial cone conformations (Figure 7). In this structure, the cation would be bound to a maximum of six oxygen donor atoms.

Variable-temperature spectra were also recorded on the cesium complex of **9**. Similar to $8\cdot\text{Rb}^+$, its spectrum at 193 K is similar to that at 291 K, indicating that the cation is tightly bound within the ligand as would be expected based upon the crystal structure of $9\cdot\text{CsClO}_4$ (Figure 3).

These experiments are consistent with the modeling results, both showing that the smaller sodium cation cannot bind simultaneously to all eight donor atoms in **8**, whereas the larger rubidium cation is able to do so. This fact accounts for **8** not binding Na^+ in the competitive 99:1 DMSO:water solvent mixture (Table 1). The same situation also occurs for ligand **9** where the larger alkali metal cations, in particular, Cs^+ and Rb^+ , can effectively bind to all oxygen donor atoms, but the smaller cations cannot and thus are not bound.

Analogous VT ^1H NMR experiments were performed on pyridylene ligand **11** with sodium and cesium cations in acetone- d_6 over the temperature range from 290 to 193 K. The room-temperature spectrum of $11\cdot\text{Na}^+$ is quite sharp and simple, indicating either that the cation is rapidly shuttling within the molecule or that it is complexed in a symmetric manner. As

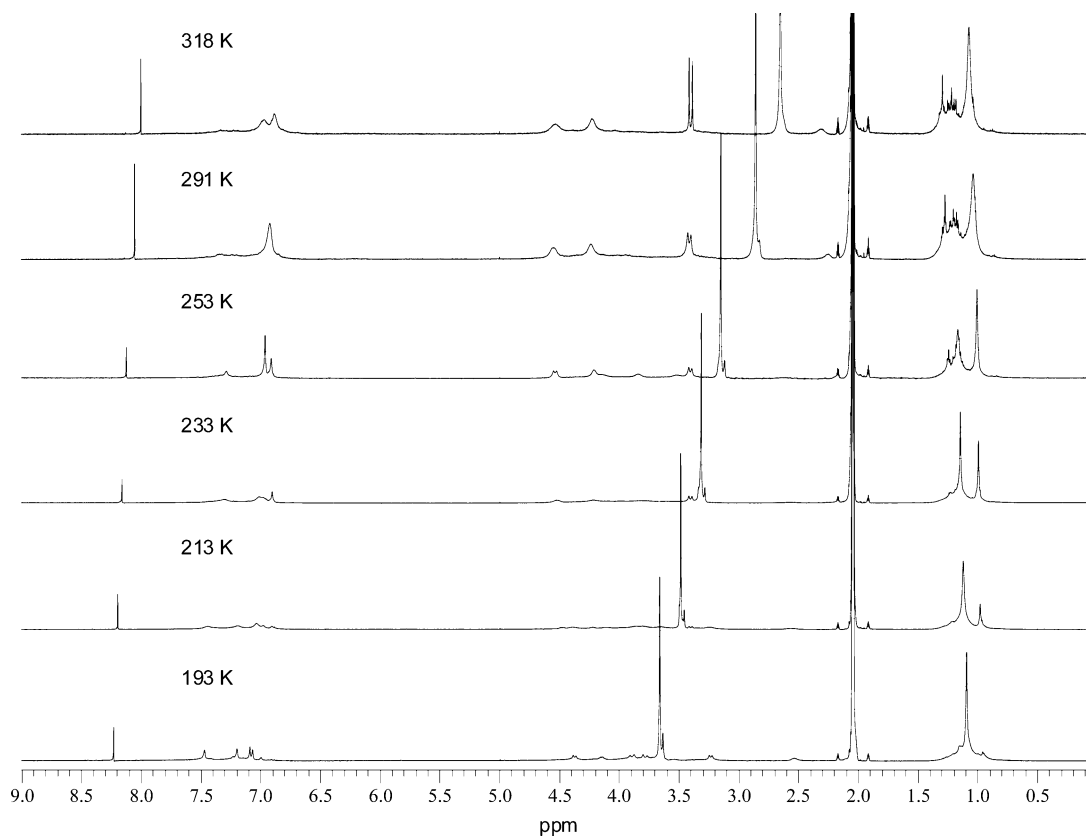


Figure 6. Variable-temperature ^1H NMR spectra of the sodium ion complex of **8** in the range from 318 to 193 K (500 MHz, acetone- d_6).

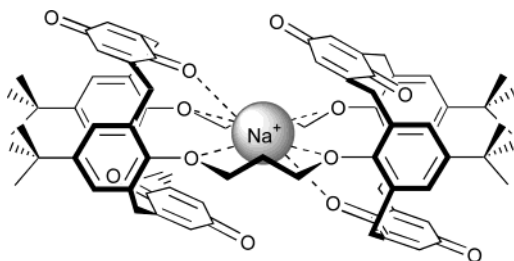


Figure 7. The predicted binding mode of Na^+ by **8** at 193 K.

the temperature is lowered, the spectrum begins to broaden and then sharpens in the range from 213 to 193 K, with the final spectrum being highly complicated. The number and position of the signals point to the presence of an asymmetrically bound complex in which the two calix[4]diquinone units are inequivalent.

The ^1H NMR spectral characteristics of the $\mathbf{11}\cdot\text{Cs}^+$ complex over the same temperature range are comparable to those of $\mathbf{11}\cdot\text{Na}^+$, which suggests that even the larger Cs^+ cation is unable to bind effectively to all of the available donor atoms. Molecular modeling studies performed on the bis(calix[4]arene) precursor **6** with group 1 cations by Marchand and co-workers²⁰ revealed that the geometry optimized structures with sodium and potassium cations involved coordination to the pyridine ring nitrogens only and any attempt to coordinate the cation to additional sites resulted in significantly higher complexation energies. For binding to involve interaction with the pyridylene nitrogens and four phenolic oxygens, the calculated total energy of the complex decreases with increasing size of the alkali metal cation

guest. The same argument can be applied to **11**; the small sodium cation is not bound in competitive 1:1 dichloromethane:DMSO solution due to it being unable to coordinate sufficiently strongly to the pyridylene nitrogens and the calix[4]diquinone oxygens donors. For K^+ , Rb^+ , and Cs^+ , as the cation size increases, coordination to both sets of donor atoms becomes more effective, resulting in a greater stability constant value (Table 1).

Electrochemical Properties

There have been several studies on the redox properties of calixquinones^{4a,15} and their recognition of cations²¹ and anions.²² Simple calix[4]diquinones can in theory accept a total of four electrons to become a tetraanion. For such species, three redox processes are generally observed in their cyclic (CV) and square wave (SWV) voltammograms. The first two couples occur at similar potential and are assigned to one-electron transfers to each of the quinone units, giving semiquinone species. The precise potential of these two couples depends on the donor ability of the appended group on the aromatic rings, while their difference in potential reflects the interaction energy between the two added electrons in the diametrical quinone rings. This interaction energy strongly depends on the conformational properties of the ligand in solution. The third more negative wave is believed to be due to the third and fourth electron

(20) Marchand, A. P.; Chong, H.-S.; Takhi, M.; Power, T. D. *Tetrahedron* **2000**, *56*, 3121.

(21) (a) Choi, D.; Chung, T. D.; Kang, S. K.; Lee, S. K.; Kim, T.; Chang, S.-K.; Kim, H. *J. Electroanal. Chem.* **1995**, *387*, 133. (b) Gómez-Kaifer, M.; Reddy, P. A.; Gutsche, C. D.; Echegoyen, L. *J. Am. Chem. Soc.* **1994**, *116*, 3580. (c) Chen, Z.; Gale, P. A.; Heath, J. A.; Beer, P. D. *J. Chem. Soc., Faraday Trans.* **1994**, *90*, 293.

(22) (a) Nam, K. C.; Kang, S. O.; Jeong, H. S.; Jeon, S. *Tetrahedron Lett.* **1999**, 7343. (b) Jeong, H.; Choi, E. M.; Kang, S. O.; Nam, K. C.; Jeon, S. *J. Electroanal. Chem.* **2000**, *485*, 154.

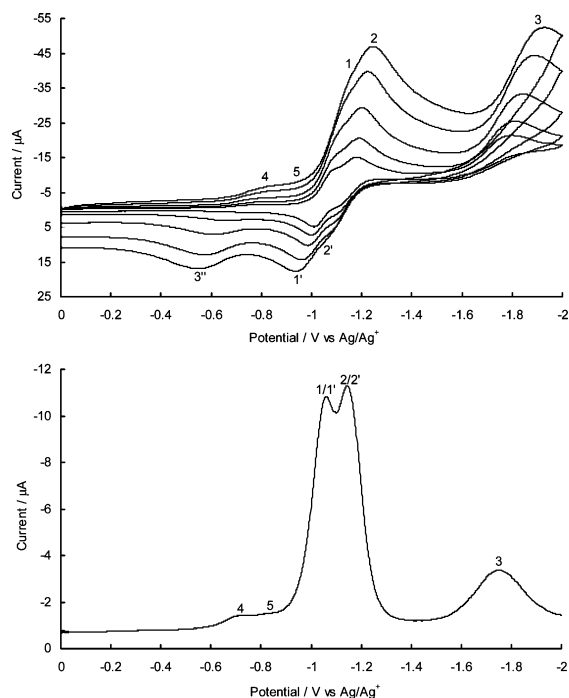


Figure 8. CVs (top) at various scan rates (in order of increasing amplitude of current: 50, 100, 200, 400, and 600 mV s^{-1}) and SWV (bottom) (5 Hz) of **9** in 4:1 $\text{CH}_2\text{Cl}_2:\text{CH}_3\text{CN}$.

Table 3. Electrochemical Data^a in 4:1 $\text{CH}_2\text{Cl}_2:\text{CH}_3\text{CN}$

| redox couple or wave/V | 8 | 9 | 10 | 11 |
|------------------------|----------|----------|-----------|-----------|
| $E_{1/2}$ (1/1') | -1.04 | -1.06 | -1.06 | -1.04 |
| $E_{1/2}$ (2/2') | -1.16 | -1.15 | -1.18 | -1.14 |
| E_{pc} (3) | -1.70 | -1.75 | -1.78 | -1.64 |

^a 0.1 M *n*-Bu₄NBF₄ was added as the supporting electrolyte. The concentration of the receptor in the solution was approximately 1×10^{-3} M. Maximum errors estimated to be ± 10 mV. $E_{1/2}$ values are the averages of the cathodic and anodic peak potentials of the described couple referenced to an Ag/Ag⁺ electrode at 298 K. E_{pc} is the cathodic peak potential of wave 3, which is irreversible.

transfers. Casnati and co-workers suggested that the irreversibility of this wave could be due to the formation of insoluble hydroquinone species.¹⁵

The electrochemistry of the bis(calix[4]diquinone) ligands **8**–**11** was investigated in 4:1 dichloromethane:acetonitrile using cyclic and square wave voltammetric techniques. The experiments revealed that these four ligands exhibit very similar electrochemical properties that are comparable to those of the simple calix[4]diquinones. The receptors all show three redox waves in their voltammograms, two of which are close together and reversible, 1/1' and 2/2', and the other wave, 3, occurring at a considerably more negative potential, being irreversible. In a simple calix[4]diquinone, redox couples 1/1' and 2/2' are considered to be two one-electron processes, and wave 3 is considered to be a two-electron reduction process; it is, therefore, logical to conclude that in the bis(calix[4]diquinone) ligands, couples 1/1' and 2/2' are two two-electron processes, and wave 3 is a four-electron reduction. Again, the irreversibility of wave 3 may be due to the formation of insoluble hydroquinone species.

Propylene ligand **8** exhibits essentially the same CV and SWV as pentylene ligand **10**. Butylene **9** and pyridylene **11** receptors display CVs and SWVs similar to those of **8** under the same

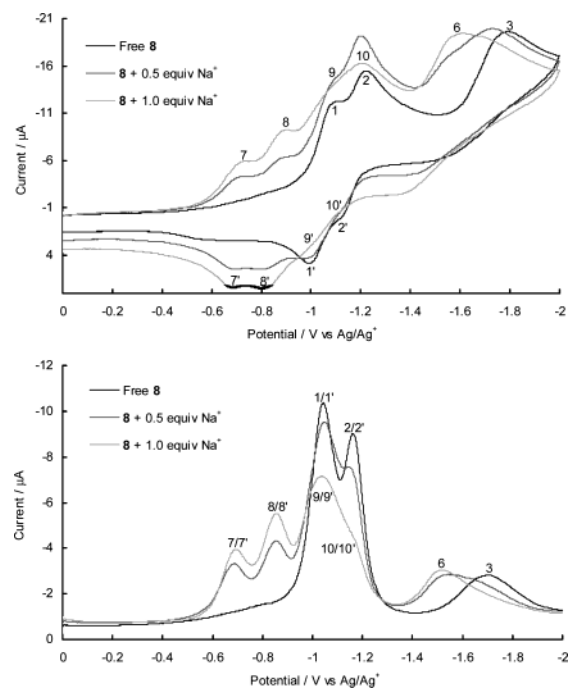


Figure 9. CVs (top) (100 mV s^{-1}) and SWVs (bottom) (5 Hz) of **8** free and in the presence of Na⁺ cations in 4:1 $\text{CH}_2\text{Cl}_2:\text{CH}_3\text{CN}$.

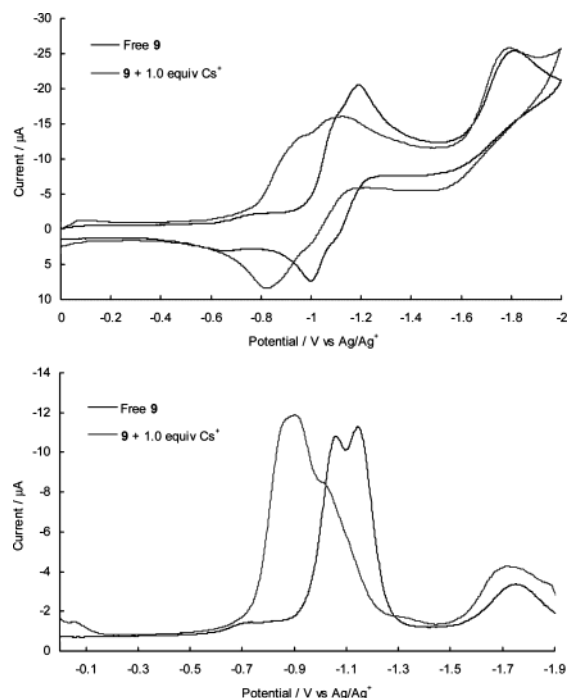
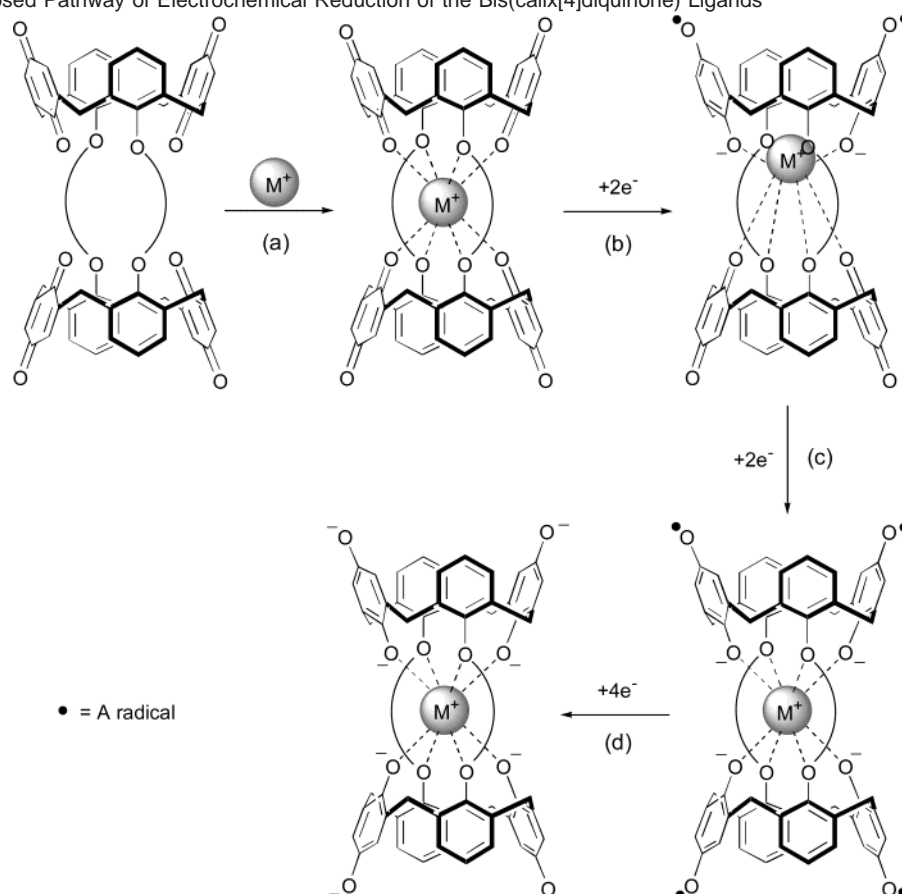


Figure 10. CVs (top) (100 mV s^{-1}) and SWVs (bottom) (5 Hz) of **9** free and in the presence of Cs⁺ cations in 4:1 $\text{CH}_2\text{Cl}_2:\text{CH}_3\text{CN}$.

conditions, except that **9** and **11** also show prewave couples 4 and 5 (Figure 8).^{4a} The half-wave potentials of couples 1/1' and 2/2', and the reduction potential of wave 3, are summarized in Table 3. Ligand **9** also displays a wave 3'', the occurrence of which in simple calix[4]diquinones has been attributed to incompletely protonated quinone dianion species.^{21c}

The alkali metal cation electrochemical recognition properties of the bis(calix[4]diquinone) receptors **8**–**11** have been investigated by cyclic and square wave voltammetry through the addition of group 1 cations to electrochemical solutions of the

Scheme 2. The Proposed Pathway of Electrochemical Reduction of the Bis(calix[4]diquinone) Ligands

respective receptor in a 4:1 dichloromethane:acetonitrile solvent mixture. The preformed ethylene-bridged complex **7**·KPF₆ was examined in acetonitrile solution.

The electrochemical properties of the bis(calix[4]diquinone)/alkali metal cation complexes are significantly more complicated than those of simple calix[4]diquinone ligands.^{4a} Typically, upon addition of 1 equiv or more of cation, the original redox couples 1/1' and 2/2' disappeared, giving rise to the appearance of four or three (one of which is broad, implying two overlapping couples) new reversible redox couples; two of these new couples, 7/7' and 8/8', are substantially anodically shifted as compared to the original couples 1/1' and 2/2', while the other one or two new waves, 9/9' and 10/10', occur at a potential similar to that of 1/1' and 2/2'. The irreversible wave 3 in the free ligand is also seen to shift anodically and is labeled as wave 6 in the complex. Examples of these phenomena are shown in Figures 9 and 10, the CVs and SWVs of **8** with sodium cations and **9** with cesium cations, respectively.

The observed metal cation electrochemical recognition behavior of the receptors can be tentatively rationalized by the processes displayed in Scheme 2. The first step involves complexation of the cation by the ligand. In stage b, it is assumed that electron transfer to one of the calix[4]diquinone moieties proceeds earlier in real time than to the second calix[4]diquinone. As soon as the first reduction occurs, the complexed cation moves to an asymmetric positioning in the molecule, closer to the reduced end due to the strong electrostatic interaction between anion and cation. These two reductions account for couples 7/7' and 8/8'. In the following stage c, two further one-electron reductions occur at the neutral calixdiqui-

none moiety. Because of the cation being closer to the negatively charged calixdiquinone unit, however, the reductions giving rise to couples 9/9' and 10/10' occur at a less anodically shifted potential, in fact occurring at around the same potential as couples 1/1' and 2/2'. The final reductions, occurring in stage d, effectively give rise to the broad wave 6 which is anodically shifted from the original wave 3, as expected. A summary of the electrochemical data for all of the ligands with 1 equiv of each group 1 cation is displayed in Table 4.

The magnitude of the anodic shifts of the redox couples 7/7' and 8/8' can be seen to reflect the polarizing power of the cation involved, with Na⁺ producing the largest shift and Cs⁺ producing the smallest (for the 7/7' couple of **9**, for example, shifts of 330 mV with Na⁺ and 190 mV with Cs⁺ are observed). The shifts of the couples 9/9' and 10/10', however, do not seem to follow any obvious trend. It is noteworthy that electrochemical competition experiments with **9** in a mixture of 4:1 dichloromethane:acetonitrile in the presence of a 10-fold excess amount of sodium cations did not affect the receptors selective response to cesium ions.

With ligand **10**, the addition of K⁺, Rb⁺, and Cs⁺ cations only produced minor perturbations in voltammetric behavior, which is a reflection of the weak alkali metal cation coordination properties of this ligand.

Conclusion

The bis(calix[4]diquinone) series of ligands containing either alkylene or pyridylene bridges are redox-active molecules that possess unique three-dimensional, donor atom lined cavities and represent a new design of ionophore capable of electrochemical

recognition. All of these hosts can be synthesized in just two steps from *tert*-butylcalix[4]arene. Stability constant determinations with alkali metal cations revealed that the length and nature of the bridging chain between the two calix[4]diquinone moieties crucially dictate the selectivity and strength of group 1 metal cation binding. Whereas a propylene linkage bestows rubidium ion selectivity upon the host, the presence of the longer butylene spacers allows for selective cesium ion complexation; in particular, a large Cs⁺/Na⁺ preference is observed. An X-ray crystal structure of the cesium complex of butylene-bridged bis(calix[4]diquinone) **9** illustrates that the cation resides within the cavity bonded to all eight oxygen donor atoms. Molecular modeling, based on these X-ray data, shows that the cavity size of butylene-bridged host **9** is highly complementary to the cesium ion. A combination of variable-temperature ¹H NMR and molecular dynamics studies has shown that for the alkylene-linked hosts, effective binding is only observed for systems in which the metal cation can simultaneously bind to all eight oxygen donor atoms. The host bearing pyridylene spacers **11** also displays cesium ion selectivity, a consequence of this cation being able to coordinate more effectively than the other metal cations to the available donors. These redox-active receptors exhibit substantial electrochemical recognition effects toward group 1 metal cations. Electrochemical competition experiments reveal the butylene-linked receptor **9** is capable of selectively sensing cesium ion in the presence of excess amounts of sodium cations. This observation is of real significance and demonstrates this ionophore's potential use as a novel amperometric cesium ion sensor.

Experimental Section

All chemicals were commercial grade and used without further purification unless otherwise stated. Solvents were predried, purified by distillation, and stored under nitrogen where appropriate.

Nuclear magnetic resonance spectra were recorded using either a 300 MHz Varian VXWorks spectrometer or a 500 MHz Varian Unity spectrometer. FAB mass spectral analyses were carried out by the EPSRC mass spectrometry service of University College, Swansea. Electrospray mass spectra were recorded using Micromass LCT equipment. Microanalyses were obtained on an elemental vario EL and were performed by the Inorganic Chemistry Laboratory, University of Oxford.²³ Electrochemical measurements were carried out using an EG&G Princeton Applied Research 273 potentiostat/galvanostat. All reported voltammograms were recorded on the first potential sweep. The electrochemical cell was an unsealed one compartment cell with a glassy carbon working electrode, an Ag/Ag⁺ reference electrode (0.33 V ± 10 mV vs SCE), and a Pt wire coil counter electrode. The reference contained an internal solution of 0.01 M AgNO₃ and 0.1 M *n*-Bu₄NBF₄ in acetonitrile and was incorporated with a salt bridge containing 0.1 M TBABF₄ in the respective solvent. All electrochemical solutions were degassed with argon and maintained under an argon atmosphere for the duration of the experiment. Kemet diamond sprays (1 μm and 0.25 μm) were used to polish the working electrode. UV/Vis spectra were obtained using a PC-controlled Perkin-Elmer Lambda 6 spectrometer. *p*-*tert*-Butylcalix[4]arene,²⁴ ethane-1,2-ditosylate, propane-1,3-ditosylate,²⁵ bis(bromomethyl)pyridine,²⁶ and Ti(OOCF₃)₃ in TFA^{14b} were prepared according to literature procedures.

General Procedure for the Synthesis of Bis(calix[4]arene) Molecules 2–6. A suspension of *p*-*tert*-butylcalix[4]arene (4.0 g, 6.2 mmol) and K₂CO₃ (0.94 g, 6.8 mmol) in acetonitrile (100–200 mL) was refluxed for 2 h. After this time, the respective alkylating agent (ethane-1,2-ditosylate, propane-1,3-ditosylate, 1,4-dibromobutane, 1,5-dibromopentane, or 2,6-bis(bromomethyl)pyridine) (7.4 mmol) was added, and the mixture was refluxed for a further 2–3 days. Following removal of the solvent in vacuo, the mixture was partitioned between chloroform (150 mL) and water (150 mL). The organic layer was dried (MgSO₄) and reduced in vacuo.

Doubly Ethylene-Bridged Bis(calix[4]arene) (2). To this crude material was added ethanol (120 mL), which after briefly refluxing, was hot-filtered, affording **2** as a colorless powder (2.21 g, 53%). ¹H NMR (500 MHz, CDCl₃): δ 1.01 (s, 36H, (CH₃)₃C), 1.27 (s, 36H, (CH₃)₃C), 3.38 (d, ²J = 12.5 Hz, 8H, ArCH₂Ar), 4.52 (d, ²J = 12.5 Hz, 8H, ArCH₂Ar), 4.62 (s, 8H, OCH₂CH₂O), 6.88 (s, 8H, ArH), 7.01 (s, 8H, ArH), 7.71 (s, 4H, OH). ¹³C NMR (75 MHz, CDCl₃): δ 31.12 ((CH₃)₃C), 31.77 ((CH₃)₃C), 32.48 (ArCH₂Ar), 33.81 ((CH₃)₃C), 33.98 ((CH₃)₃C), 75.91 (OCH₂CH₂O), 124.81, 125.55, 127.70, 132.35, 140.72, 146.38, 150.98, and 151.35 (Ar). MS (FAB): *m/z* 1350 [M], 1373 [M + Na]. Anal. Calcd for C₉₂H₁₁₆O₈: C, 81.86; H, 8.66. Found: C, 81.07; H, 9.25.

Doubly Propylene-Bridged Bis(calix[4]arene) (3). To this crude material was added ethanol (125 mL), which after briefly refluxing, was hot-filtered, affording **3** as an analytically pure, colorless powder (1.24 g, 30%). ¹H NMR (300 MHz, CDCl₃): δ 1.20 (s, 36H, (CH₃)₃C), 1.23 (s, 36H, (CH₃)₃C), 3.10 (quin, ³J = 8.2 Hz, 4H, OCH₂CH₂CH₂O), 3.40 (d, ²J = 12.9 Hz, 8H, ArCH₂Ar), 4.32 (t, ³J = 8.2 Hz, 8H, OCH₂CH₂CH₂O), 4.44 (d, ²J = 12.9 Hz, 8H, ArCH₂Ar), 7.02 (s, 8H, ArH), 7.09 (s, 8H, ArH), 8.88 (s, 4H, OH). ¹³C NMR (75 MHz, CDCl₃): δ 30.86 (OCH₂CH₂CH₂O), 31.29 ((CH₃)₃C), 31.64 ((CH₃)₃C), 32.78 (ArCH₂Ar), 33.84 ((CH₃)₃C), 34.23 ((CH₃)₃C), 72.65 (OCH₂CH₂CH₂O), 125.23, 125.87, 127.88, 133.83, 141.48, 147.27, 149.63, and 150.43 (Ar). MS (FAB): *m/z* 1378 [M], 1401 [M + Na]. Anal. Calcd for C₉₄H₁₂₀O₈·¹/₃(CHCl₃): C, 79.94; H, 8.56. Found: C, 79.95; H, 8.75.

Doubly Butylene-Bridged Bis(calix[4]arene) (4). To this crude material was added acetonitrile (150 mL), and the resulting suspension was refluxed for around 10 min. Subsequent hot-filtering afforded **4** as a colorless powder in around 90% purity (1.01 g, 23%). Further purification could be achieved, if necessary, by recrystallization via slow evaporation from methanol/dichloromethane. ¹H NMR (300 MHz, CDCl₃): δ 1.10 (s, 36H, (CH₃)₃C), 1.23 (s, 36H, (CH₃)₃C), 2.65 (br m, 8H, OCH₂CH₂CH₂CH₂O), 3.20 (d, ²J = 13.0 Hz, 8H, ArCH₂Ar), 4.15 (br m, 8H, OCH₂(CH₂)₂CH₂O), 4.34 (d, ²J = 13.0 Hz, 8H, ArCH₂Ar), 6.89 (s, 8H, ArH), 6.95 (s, 8H, ArH), 8.41 (s, 4H, OH). ¹³C NMR (75 MHz, CDCl₃): δ 25.42 (OCH₂CH₂CH₂CH₂O), 31.22 ((CH₃)₃C), 31.77 ((CH₃)₃C), 32.02 (ArCH₂Ar), 33.75 ((CH₃)₃C), 34.13 ((CH₃)₃C), 74.81 (OCH₂(CH₂)₂CH₂O), 124.71, 125.52, 127.24, 133.39, 140.84, 146.71, 149.70, and 150.59 (Ar). MS (ES): *m/z* 1429 [M + Na], 1445 [M + K]. Anal. Calcd for C₉₆H₁₂₄O₈·¹/₂(CH₂Cl₂): C, 80.02; H, 8.70. Found: C, 79.95; H, 8.84.

Doubly Pentylene-Bridged Bis(calix[4]arene) (5). To this crude material was added ethanol (350 mL), and the resulting suspension was refluxed briefly. The solid was filtered off and washed with a further 100 mL of hot ethanol, affording **5** as a colorless powder (1.16 g, 26%). ¹H NMR (500 MHz, CDCl₃): δ 1.13 (s, 36H, (CH₃)₃C), 1.20 (s, 36H, (CH₃)₃C), 2.04 (quin, ³J = 8.0 Hz, 4H, O(CH₂)₂CH₂(CH₂)₂O), 2.37 (m, 8H, OCH₂CH₂CH₂CH₂CH₂O), 3.34 (d, ²J = 13.0 Hz, 8H, ArCH₂Ar), 4.06 (t, ³J = 7.5 Hz, 8H, OCH₂(CH₂)₃CH₂O), 4.34 (d, ²J = 13.0 Hz, 8H, ArCH₂Ar), 7.02 (s, 8H, ArH), 7.04 (s, 8H, ArH), 8.78 (s, 4H, OH). ¹³C NMR (75 MHz, CDCl₃): δ 21.62 (O(CH₂)₂CH₂(CH₂)₂O), 30.05 (OCH₂CH₂CH₂CH₂CH₂O), 31.22 ((CH₃)₃C), 31.62 ((CH₃)₃C), 32.40 (ArCH₂Ar), 33.80 ((CH₃)₃C), 34.15 ((CH₃)₃C), 75.87 (OCH₂(CH₂)₃CH₂O), 125.22, 125.75, 128.03, 133.68, 141.54, 147.14, 149.90, and 150.61 (Ar). MS (ES): *m/z* 1457 [M + Na], 1473 [M + K]. Anal.

(23) Problems associated with microanalysis of calixarenes have been previously reported: (a) Böhrer, V.; Jung, K.; Schön, M.; Wolff, A. *J. Org. Chem.* **1992**, *57*, 790. (b) Gutsche, C. D.; See, K. A. *J. Org. Chem.* **1992**, *57*, 4527.

(24) Gutsche, C. D.; Iqbal, M. *Org. Synth.* **1990**, *68*, 234–237.

(25) Buttafava, A.; Fabbrizzi, L.; Perotti, A.; Poggi, A.; Poli, G.; Seghi, B. *Inorg. Chem.* **1986**, *25*, 1456.

(26) Reppy, M. A.; Cooper, M. E.; Smithers, J. L.; Gin, D. L. *J. Org. Chem.* **1999**, *64*, 4191.

Table 4. Electrochemical Data^a of **7** in CH₃CN and **8–11** in 4:1 CH₂Cl₂:CH₃CN, in the Presence of 1 equiv of Group 1 Cations

| | redox couple or wave/V | 7 | 8 | 9 | 10 | 11 |
|-----------------|------------------------------------|-------|--------------------|--------------------|-------------|--------------------|
| Na ⁺ | <i>E</i> _{1/2} (7/7') | | -0.69 | -0.73 | -0.64 | -0.63 |
| | <i>E</i> _{1/2} (8/8') | | -0.86 | -0.82 | -0.73 | -0.73 |
| | <i>E</i> _{1/2} (9/9') | | -1.04 | -1.08 | -0.80 | -0.79 |
| | <i>E</i> _{1/2} (10/10') | | -1.14 ^c | -1.15 | -1.05/-1.19 | -0.98/-1.14 |
| | <i>E</i> _{pc} (6) | | -1.60 | -1.72 | -1.60 | -1.61 |
| | Δ <i>E</i> (7/7') ^b /mV | | 350 | 330 | 420 | 410 |
| K ⁺ | <i>E</i> _{1/2} (7/7') | -0.85 | -0.79 | -0.81 | <i>f</i> | -0.82 |
| | <i>E</i> _{1/2} (8/8') | -0.95 | -0.93 ^d | -0.90 | <i>f</i> | -0.91 |
| | <i>E</i> _{1/2} (9/9') | -1.05 | | -1.05 ^e | <i>f</i> | -1.06 |
| | <i>E</i> _{1/2} (10/10') | | | | <i>f</i> | -1.14 |
| | <i>E</i> _{pc} (6) | -1.76 | -1.79 | -1.72 | -1.64 | -1.65 |
| | Δ <i>E</i> (7/7') ^b /mV | | 250 | 250 | <i>f</i> | 220 |
| Rb ⁺ | <i>E</i> _{1/2} (7/7') | | -0.79 | -0.85 | <i>f</i> | -0.81 |
| | <i>E</i> _{1/2} (8/8') | | -0.92 | -0.90 | <i>f</i> | -0.93 |
| | <i>E</i> _{1/2} (9/9') | | -0.99 ^e | -1.07 | <i>f</i> | -1.05 |
| | <i>E</i> _{1/2} (10/10') | | | -1.11 | <i>f</i> | -1.12 |
| | <i>E</i> _{pc} (6) | | -1.80 | -1.74 | -1.60 | -1.65 |
| | Δ <i>E</i> (7/7') ^b /mV | | 250 | 210 | <i>f</i> | 230 |
| Cs ⁺ | <i>E</i> _{1/2} (7/7') | | -0.80 | -0.87 | <i>f</i> | -0.82 |
| | <i>E</i> _{1/2} (8/8') | | -0.94 ^e | -0.91 | <i>f</i> | -0.92 |
| | <i>E</i> _{1/2} (9/9') | | | -1.01 ^e | <i>f</i> | -1.07 ^e |
| | <i>E</i> _{1/2} (10/10') | | | | <i>f</i> | |
| | <i>E</i> _{pc} (6) | | -1.71 | -1.79 | <i>g</i> | -1.68 |
| | Δ <i>E</i> (7/7') ^b /mV | | 240 | 190 | <i>f</i> | 220 |

^a 0.1 M *n*-Bu₄NBF₄ was added as the supporting electrolyte. The concentration of the receptor in the solution was approximately 1 × 10⁻³ M. Maximum errors estimated to be ±10 mV. *E*_{1/2} values are the averages of the cathodic and anodic peak potentials of the described couple referenced to an Ag/Ag⁺ electrode at 298 K. *E*_{pc} is the cathodic peak potential. ^b Anodic shifts of the new 7/7' redox couple relative to the original redox couple 1/1'. ^c Approximate. ^d Very broad. ^e Broad. ^f Insignificant changes. ^g Not recorded.

Calcd for C₉₈H₁₂₈O₈·1/3(CHCl₃): C, 80.13; H, 8.78. Found: C, 80.66; H, 9.11.

Doubly Pyridylene-Bridged Bis(calix[4]arene) (6). To this crude material was added ethanol (90 mL), which after briefly refluxing, was hot-filtered, affording **6** as an analytically pure, colorless powder. A further small crop of product could be obtained by reducing the filtrate in vacuo and passing the residue down a short path of silica gel eluting with 7:3 (v/v) dichloromethane:hexane (1.43 g, 31% combined). ¹H NMR (300 MHz, CDCl₃): δ 1.09 (s, 36H, (CH₃)₃C), 1.28 (s, 36H, (CH₃)₃C), 3.38 (d, ²*J* = 13.2 Hz, 8H, ArCH₂Ar), 4.50 (d, ²*J* = 12.6 Hz, 8H, ArCH₂Ar), 5.16 (s, 8H, OCH₂PyCH₂O), 6.98 (s, 8H, ArH), 7.06 (s, 8H, ArH), 7.36 (t, ³*J* = 7.8 Hz, 2H, py-*p*-H), 7.99 (s, 4H, OH), 8.33 (d, ³*J* = 7.8 Hz, 4H, py-*m*-H). ¹³C NMR (75 MHz, CDCl₃): δ 31.08 ((CH₃)₃C), 31.69 ((CH₃)₃C), 32.38 (ArCH₂Ar), 33.81 ((CH₃)₃C), 34.06 ((CH₃)₃C), 78.21 (OCH₂PyCH₂O), 121.80, 125.26, 125.94, 127.40, 132.98, 137.77, 141.40, 147.12, 149.82, 150.90, and 156.30 (Ar, Py). MS (ES): *m/z* 1505 [M + H], 1527 [M + Na], 1543 [M + K]. Anal. Calcd for C₁₀₂H₁₂₂O₈N₂·1/3(CHCl₃): C, 79.61; H, 7.99; N, 1.81. Found: C, 79.90; H, 8.13; N, 2.82.

General Procedure for the Synthesis of Bis(calix[4]diquinones) 7–11. The respective bis(calix[4]arene) (0.73 mmol) was stirred in Ti(OOCF₃)₃/TFA solution (10.0 mL, 8.7 mmol) for 3 h in the dark. Approximately 90% of the TFA was then removed in vacuo, and the remainder was poured into ice water (100 mL). The product was extracted with chloroform (1 × 100 mL, 1 × 50 mL), and the combined organic extracts were washed with water (2 × 100 mL). After the organic layer (MgSO₄) was dried, the solvent was removed in vacuo.

Doubly Ethylene-Bridged Bis(calix[4]diquinone) (7). The residue was purified by column chromatography on silica gel (10 cm depth) gradient eluting from 4:1 to 3:1 (v/v) hexane:acetone. The slowest moving band, which contains **7**, was removed with 9:1 (v/v) acetone: methanol and reduced in vacuo. The residue was dissolved in chloroform (30 mL) and washed with water (30 mL). The organic layer

was reduced in vacuo, and acetonitrile (20 mL) was added to the dark orange residue. Subsequent heating and hot-filtering yielded pure **7** as a yellow, sparingly soluble powder (8%). ¹H NMR (500 MHz, CDCl₃): δ 1.28 (s, 36H, (CH₃)₃C), 3.01 (d, ²*J* = 14.0 Hz, 8H, ArCH₂-Qu), 4.40 (s, 8H, OCH₂CH₂O), 4.53 (d, ²*J* = 14.0 Hz, 8H, ArCH₂Qu), 5.89 (s, 8H, QuH), 7.12 (s, 8H, ArH). MS (ES): *m/z* 1220 [M + K]. Anal. Calcd for C₇₆H₇₆O₁₂·3/4(CHCl₃): C, 72.53; H, 6.09. Found: C, 72.56; H, 6.34.

Doubly Propylene-Bridged Bis(calix[4]diquinone) (8). The residue was purified by column chromatography on a short path of silica gel eluting with 7:3 (v/v) chloroform:ethyl acetate. Pure bis(calix[4]-diquinone) was obtained by recrystallization from chloroform/methanol as short orange needles (28%). ¹H NMR (300 MHz, CDCl₃): δ 1.26 (s, 36H, (CH₃)₃C), 2.53 (quin, ³*J* = 7.5 Hz, 4H, OCH₂CH₂CH₂O), 3.19 (d, ²*J* = 14.1 Hz, 8H, ArCH₂Qu), 3.95 (t, ³*J* = 7.5 Hz, 8H, OCH₂-CH₂CH₂O), 4.30 (d, ²*J* = 14.1 Hz, 8H, ArCH₂Qu), 6.38 (s, 8H, QuH), 7.07 (s, 8H, ArH). ¹³C NMR (75 MHz, CDCl₃): δ 29.38 (OCH₂CH₂-CH₂O), 31.23 (ArCH₂Qu), 31.47 ((CH₃)₃C), 34.29 ((CH₃)₃C), 71.48 (OCH₂CH₂CH₂O), 126.79, 132.17, 132.31, 147.07, 149.25, 152.72 (Qu, Ar), 184.96 (C=O), 187.72 (C=O). MS (ES): *m/z* 1249 [M + K]. Anal. Calcd for C₇₈H₈₀O₁₂·2/3(CHCl₃): C, 73.30; H, 6.31. Found: C, 73.72; H, 6.10.

Doubly Butylene-Bridged Bis(calix[4]diquinone) (9). The residue was purified by column chromatography on a 14 cm depth of silica gel eluting with 98:2 (v/v) chloroform:methanol, collecting the final streaking band by stripping the column with 10% methanol. To this impure final band was added a small volume of acetonitrile, and the suspension was gently heated. On cooling, a yellow powder was isolated and dissolved in chloroform (20 mL) and washed with water (2 × 20 mL). Reduction in vacuo afforded the pure product as a yellow powder (10%). ¹H NMR (500 MHz, CDCl₃): δ 1.19 (s, 36H, (CH₃)₃C), 1.85 (s, 8H, OCH₂CH₂CH₂CH₂O), 3.07 (d, ²*J* = 14.0 Hz, 8H, ArCH₂Qu), 3.86 (s, 8H, OCH₂(CH₂)₂CH₂O), 4.18 (d, ²*J* = 13.5 Hz, 8H, ArCH₂-Qu), 6.20 (s, 8H, QuH), 7.00 (s, 8H, ArH). ¹³C NMR (75 MHz, CDCl₃): δ 26.34 (OCH₂CH₂CH₂CH₂O), 30.38 (ArCH₂Qu), 31.42 ((CH₃)₃C), 34.13 ((CH₃)₃C), 73.80 (OCH₂(CH₂)₂CH₂O), 126.76, 131.80, 132.40, 146.43, 149.31, 153.64 (Qu, Ar), 185.12 (C=O), 187.95 (C=O). MS (ES): *m/z* 1261 [M + Na], 1277 [M + K]. Anal. Calcd for C₈₀H₈₄O₁₂·7/3(CHCl₃): C, 65.23; H, 5.74. Found: C, 65.91; H, 5.65.

Doubly Pentylene-Bridged Bis(calix[4]diquinone) (10). The residue was purified by column chromatography on a 14 cm depth of silica gel gradient eluting from 5:1 to 4:1 (v/v) dichloromethane:ethyl acetate. The fractions containing a yellow spot in TLC were combined and recrystallized from acetonitrile to give the impure product. Pure compound was isolated by crystallization from chloroform/methanol via slow evaporation as yellow needles (9%). ¹H NMR (500 MHz, CDCl₃): δ 1.20 (s, 36H, (CH₃)₃C), 1.33 (br s, 4H, O(CH₂)₂CH₂-(CH₂)₂O), 1.74 (br s, 8H, OCH₂CH₂CH₂CH₂CH₂O), 3.27 (d, ²*J* = 13.5 Hz, 8H, ArCH₂Qu), 3.70 (m, 8H, OCH₂(CH₂)₃CH₂O), 4.01 (d, ²*J* = 13.5 Hz, 8H, ArCH₂Qu), 6.50 (br s, 8H, QuH), 7.01 (s, 8H, ArH). ¹³C NMR (75 MHz, CDCl₃): δ 22.60 (O(CH₂)₂CH₂(CH₂)₂O), 30.26 (ArCH₂Qu), 31.42 ((CH₃)₃C), 32.81 (OCH₂CH₂CH₂CH₂CH₂O), 34.13 ((CH₃)₃C), 72.98 (OCH₂(CH₂)₃CH₂O), 126.94, 131.41, 132.28, 146.52, 148.90, and 153.02 (Ar, Qu), 185.41 (C=O), 188.33 (C=O). MS (ES): *m/z* 1289 [M + Na], 1305 [M + K]. Anal. Calcd for C₈₂H₈₈O₁₂·3/4(CHCl₃): C, 73.34; H, 6.55. Found: C, 73.69; H, 6.37.

Doubly Pyridylene-Bridged Bis(calix[4]diquinone) (11). The residue was purified by column chromatography on silica gel (14 cm depth) gradient eluting from 98:2 to 95:5 (v/v) chloroform:methanol. The penultimate band was reduced in vacuo and rechromatographed on silica gel (15 cm depth) gradient eluting from ethyl acetate to 9:1 (v/v) ethyl acetate:MeOH. Isolation of the final band gave impure **11**, which through further purification by hot-filtering from MeOH (20 mL) and subsequent cold-filtering from CH₃CN (20 mL) gave pure **11** as a yellow powder (18%). ¹H NMR (500 MHz, CDCl₃): δ 1.17 (s, 36H, (CH₃)₃C), 3.53 (d, ²*J* = 14.5 Hz, 8H, ArCH₂Qu), 3.81 (d, ²*J* = 14.0

Hz, 8H, ArCH₂Qu), 5.04 (s, 8H, OCH₂PyCH₂O), 6.44 (s, 8H, QuH), 7.06 (s, 8H, ArH), 7.56 (d, ³J = 8.0 Hz, 4H, py-*m*-H), 7.92 (br s, 2H, py-*p*-H). ¹³C NMR (75 MHz, CDCl₃): δ 31.26 ((CH₃)₃C), 34.08 and 34.73 ((CH₃)₃C and ArCH₂Qu), 73.87 (OCH₂PyCH₂O), 122.18, 127.89, 129.27, 132.06, 138.26, 146.24, 147.73, 152.79 and 156.15 (Ar, Qu, Py), 185.75 (C=O), 187.39 (C=O). MS (ES): *m/z* 1337 [M + H], 1359 [M + Na], 1375 [M + K]. Anal. Calcd for C₈₆H₈₂O₁₂N₂·¹/₂(CHCl₃): C, 74.46; H, 5.96; N, 2.01. Found: C, 74.92; H, 5.73; N, 2.11.

Doubly Ethylene-Bridged Bis(calix[4]diquinone)·KPF₆ Complex (7·KPF₆). Ethylene-bridged bis(calix[4]diquinone) **7** (20 mg, 0.017 mmol) was suspended in a 1:1 mixture of chloroform:acetone (25 mL total), and an excess of potassium hexafluorophosphate was added. After being stirred at room temperature for 3 h, the solvents were removed in vacuo. The residue was partitioned between chloroform (20 mL) and water (20 mL). Reduction of the organic layer in vacuo yielded pure complex as a yellow powder (23 mg, 100%). ¹H NMR (500 MHz, CDCl₃): δ 0.96 (s, 36H, (CH₃)₃C), 3.12 (d, ²J = 13.0 Hz, 8H, ArCH₂-Qu), 4.32 (s, 8H, OCH₂CH₂O), 4.45 (d, ²J = 12.5 Hz, 8H, ArCH₂Qu), 6.71 (s, 16H, QuH and ArH). MS (ES): *m/z* 1220 [M + K]. Anal. Calcd for C₇₆H₇₆O₁₂KPF₆: C, 66.85; H, 5.61; K, 2.86; P, 2.27. Found: C, 66.18; H, 6.32; K, 2.90; P, 2.12.

Molecular Modeling. All simulations were carried out in the gas phase. Molecular mechanics and molecular dynamics were carried out using the Cerius 2 software package²⁷ with parameters from the Universal Force Field.²⁸ Partial atomic charges for atoms in the macrocycles were calculated using the Gasteiger method implemented in Cerius 2. Starting models were generated from the known crystal structures of **9**·Cs⁺ and **10** with atoms in the alkylene links added or subtracted where required. Molecular dynamics simulations with the cations were carried out at 300 K. The stepsize was 1.0 fs, and the simulations were carried out for 500 ps unless otherwise stated. The set of atomic positions was saved every 250 time steps (0.25 ps) leading to trajectory files with 2000 conformations collected over 500 ps. A constant NVE thermostat with default parameters was used. No M–O bonds were included so that the interactions were primarily electrostatic.

X-ray Crystal Structure Analysis of Compounds **3 and **10**.** Data were measured with Mo K α radiation using the MARresearch Image Plate System. Data analyses were carried out with the XDS program.²⁹ The structures were solved using direct methods with the Shelx86 program.³⁰ Crystal data for **3**: C₉₇H₁₂₆Cl₉O₉·5, *M_r* = 1763.03, monoclinic, spacegroup *P*2₁/*c*, *a* = 16.016(17), *b* = 37.292(44), *c* = 18.852(26) Å, β = 90.33(1)°, *U* = 11260 Å³, ρ_{calcd} = 1.040 g cm⁻³, *Z* = 4. The crystal was positioned at 90 mm from the Image Plate. One hundred frames were measured at 2° intervals with a counting time of 5 min to give 12 916 independent reflections. There were five solvent chloroform molecules, one of which was refined with full occupancy and four with

50% occupancy. In addition, there were three solvent water molecules which were refined with 50% occupancy. All non-hydrogen atoms except those in partially occupied solvent molecules were refined anisotropically. The hydrogen atoms bonded to carbon and oxygen in the macrocycle were included in geometric positions and given thermal parameters equivalent to 1.2 times those of the atom to which they were attached. The hydrogen atoms in the solvent water molecules could not be located and were not included. The structure was refined on *F*² using Shelx³¹ to *R*₁ 0.0984, *wR*₂ 0.3008 for 8820 reflections with *I* > 2 σ (*I*). Crystal data for **10**: C₉₀H₁₀₆O₁₆S₄, *M_r* = 1571.99, triclinic, spacegroup *P*-1, *a* = 13.497(17), *b* = 14.064(15), *c* = 14.010(15) Å, δ = 116.74(1), β = 99.69(1), γ = 105.31(1)°, *U* = 2160 Å³, *Z* = 1, ρ_{calcd} = 1.209 Mg m⁻³, μ = 0.174 mm⁻¹. The crystal was positioned at 70 mm from the Image Plate. One hundred frames were measured at 2° intervals with a counting time of 10 min to give 7583 independent reflections. The dimer contains a crystallographic center of symmetry. There are three independent DMSO solvent molecules, two of which were partially overlapping and refined with 50% occupancy. The non-hydrogen atoms were refined with anisotropic thermal parameters. The hydrogen atoms were included in geometric positions and given thermal parameters equivalent to 1.2 times those of the atom to which they were attached. The structures were refined on *F*² using Shelxl. The final *R* values were *R*₁ 0.1217 and *wR*₂ 0.3841 for data with *I* > 2 σ (*I*). Crystallographic data (excluding crystallographic structural factors) for **3** and **10** have been deposited with the Cambridge Crystallographic Data Centre as supplementary publication Nos. CCDC-197045 and CCDC-197046, respectively. Copies of the data can be obtained free of charge on application to The Director, CCDC, 12 Union Road, Cambridge CB2 1EZ, U.K. (Fax: int. code +1223 336-033. E-mail: deposit@chemcrs.cam.ac.uk.).

Acknowledgment. We thank the EPSRC for a studentship (P.R.A.W.) and the EPSRC and University of Reading for funds for the crystallographic image plate system. The EPSRC Mass Spectrometry Service (University College, Swansea) is gratefully acknowledged for the provision of FAB mass spectra. V.F. thanks F.C.T. for a sabbatical leave grant.

Supporting Information Available: Figures of VT ¹H NMR spectra of **8** and **11**·Na⁺, crystal structure of **9**·Cs⁺ infinite chain, variations in M–O distance during the simulations of ML⁺ for Na⁺, K⁺, Rb⁺, and Cs⁺ cations with macrocycles **8**–**10**, and CVs and SWVs of **10** in the presence of sodium cations. Table of the potentials of the redox couples of **9**–**11** in the presence of excess sodium cations (PDF), and CIF files for **3** and **10**. This material is available free of charge via the Internet at <http://pubs.acs.org>.

JA029740T

(27) Cerius2 v3.5; Molecular Simulations Inc., San Diego, CA, 1999.

(28) Rappe, A. K.; Casewit, C. J.; Colwell, K. S.; Goddard, W. A., III; Skiff, W. M. *J. Am. Chem. Soc.* **1992**, *114*, 10024–10035.

(29) Kabsch, W. *J. Appl. Crystallogr.* **1988**, *21*, 916.

(30) Sheldrick, G. M. *Acta Crystallogr.* **1990**, *A46*, 467.

(31) Sheldrick, G. M. Shelxl, program for crystal structure refinement; University of Gottingen, 1993.